Journal of Macromolecular Science, Part A
Publication details, including instructions for authors and subscription information:
http://www.informaworld.com/smpp/title~content=t713597274

Basic Concepts of Structure Formation During Processing of Thermoplastic Materials

H. Janeschitz-Kriegl[a]; G. Eder[a]
[a] Institute of Chemistry Linz University, Linz, Austria

To cite this Article Janeschitz-Kriegl, H. and Eder, G.(1990) 'Basic Concepts of Structure Formation During Processing of Thermoplastic Materials', Journal of Macromolecular Science, Part A, 27: 13, 1733 — 1756
To link to this Article: DOI: 10.1080/00222339009351512
URL: http://dx.doi.org/10.1080/00222339009351512

J. MACROMOL. SCI.—CHEM., A27(13 & 14), pp. 1733–1756 (1990)

BASIC CONCEPTS OF STRUCTURE FORMATION DURING PROCESSING OF THERMOPLASTIC MATERIALS

H. JANESCHITZ-KRIEGL and G. EDER

Institute of Chemistry
Linz University
A-4040 Linz, Austria

ABSTRACT

A report is given of progress achieved during a 5-year period for describing the solidification of polymers by crystallization. Emphasis is placed on the fact that the classical quasi-equilibrium treatment of solidification under heat transfer conditions (as known under the heading of moving boundary value problems) is unable to predict any texturing in one-component systems. For polymers which are notorious for their slow approach to thermodynamic equilibrium, the local equilibrium theories, which are popular in metallurgy, are not discussed. In the present paper we show how to cope with nucleation under changing temperature conditions. Use is made of an adaptation of Avrami's theory to nonisothermal conditions, as recently proposed. Experimental work is extended to conditions of flow, where nucleation is enhanced. We show the possibility of theoretically describing this latter phenomenon.

1. INTRODUCTION

The symposium presented in this issue is devoted to polymer blends and alloys. As happens very often in technology, the more complex situations attract attention before the basic situations are understood.

This may serve as an excuse for the introduction of the present subject which must be studied on one-component systems first, whereas most contributions to this symposium are concerned with multicomponent systems.

Structure formation is observed in connection with the following processes of solidification from the melt:

(a) Glass transition
(b) Crystallization

With multicomponent systems, more complicated situations can be expected. For instance, one can imagine that phase separation takes place and one phase changes into the glassy state, whereas the other phase remains rubbery elastic or changes into the crystalline state. Many types of composite materials are known in this field [5, 6].

In the following we restrict ourselves to solidification by crystallization. Even after this restriction, we find three typical situations:

(a) Demixing in the melt
(b) Homogeneous melt, eutectic demixing during crystallization
(c) Homogeneous melt, no demixing during crystallization, mostly the case with one-component systems

In Case (a), the ultimate texturing of the product is largely dependent on the quality of disperse mixing in the fluid state [7, 8], although the structures of the interiors of the phases may be of some additional influence.

Case (b) is very popular in metallurgy. There exists a vast literature, starting with the classical Stefan problem of 1889 [9]. A beautiful survey is given in Crank's book [10]. When phase separations occur in these systems, mass transport becomes unavoidable as a second mechanism near the transport of heat. Characteristic for the classical approach is the assumption of local thermodynamic equilibrium at the phase boundaries. This may become clear for the simple case of the solidification of seawater, which was treated by Stefan without taking notice of the salt content. Water crystallizes in the form of pure crystals. Consequently, the salt content must increase in front of the moving phase boundary. The local salt content is deduced from a solution of the additional diffusion problem, but the melting point depression which determines the crystallization temperature at the phase boundary is derived from the

local salt concentration with the aid of thermodynamic equilibrium considerations. A similar role is attributed to the classical phase diagrams in more complex situations. This is the reason why we propose to call these treatments "quasi-equilibrium treatments." They obviously apply only to materials of high-speed crystallization or to slow processes, as with Stefan's growth problems of the ice layer on the polar sea.

Confronted with Case (c), however, one observes—after some early surprises—that the classical treatment is unable to predict any texturing. As seen below, texturing in these systems is caused by nucleation as influenced by temperature and flow. In the literature mentioned in connection with Case (b), the key word "nucleation" is rarely found, however.

The assumption of local equilibrium also leads to deviating predictions of the progress of crystallization from a cold mold surface. For most polymers, this progress is terribly overestimated. The famous "square root law," describing the distance of a crystallization front from the quenched wall as a function of time, has an infinite slope at time zero, which makes it inconsistent with the conditions of a slow process. As seen below, in a correct treatment, the crystallization front departs with a finite speed characteristic for the temperature of the quenched wall. In other words, the crystallization front is permitted to be supercooled (no local equilibrium!). Consequently, an adjacent area of the melt is supercooled before the front arrives. But this is the crucial point: This fact opens the way for a dispersed nucleation in the melt, dependent on the local thermal history of the melt. With the classical treatment the melt is free of nuclei per definition: Its temperature is assumed to be at or above the melting point throughout.

In Fig. 1 a schematic representation of the situations is given. This figure holds for the quench of the equatorial plane of the semi-infinite space. As a consequence of nucleation in the melt, a crystallization zone is formed which after some time supersedes the front departing from the quenched plane.

2. CRYSTALLIZATION IN A QUIESCENT MELT

2.1. Some Orientational Experiments

The correctness of Fig. 1 is directly supported by the microphotograph shown in Fig. 2. This photograph is of a cut through a sample of polypropylene as quenched at its surface to 120°C in the indicated way.

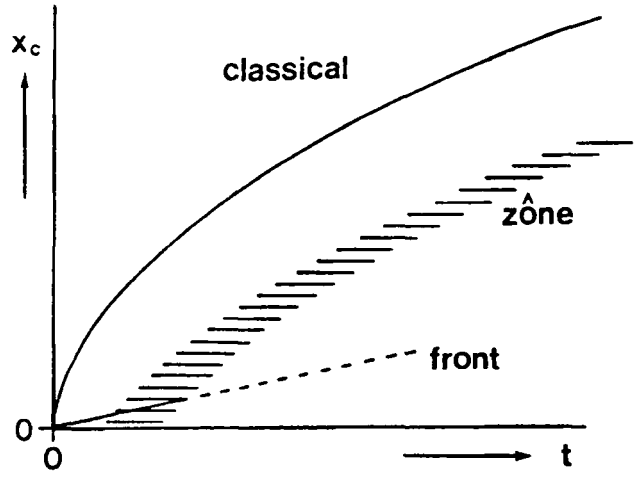

FIG. 1. Schematic presentation of the progress of crystallization into a semi-infinite body quenched at the plane where $x = 0$. Courtesy of Elsevier Applied Science Publishers, Amsterdam, Rolduc Polymer Meeting, 1989.

One recognizes an area near the quenched surface which has a striated appearance but does not show any spherulites. Apparently this area ends where it impinges with spherulites which have their growth centers at larger distances from the surface of the sample. This situation can be exaggerated by quenching the sample in two steps. First, the sample surface is quenched from a temperature well above the melting point to a temperature not too far below the melting point. Under such moderate supercooling, nucleation in the bulk of the melt is not very active, so that the front departing from the surface gets its chance to proceed. After a certain "contact time" at this first temperature, a second quench to a rather low temperature is initiated. As a consequence, the front is "frozen in" and material lying before this front forms a fine grained structure, shown in Fig. 3. By carrying out a series of these experiments with varying "contact times," one obtains a curve showing the progress of this front with time. The initial slope of this curve gives the speed of the front at the temperature of the quenched wall. This has been shown by Eder and Janeschitz-Kriegl [11] in their treatment of the crystallization front. In Fig. 4 these front speeds are gathered for two types of industrial polypropylenes, one with a more narrow and the other with the usual broad molecular weight distribution (full symbols) according

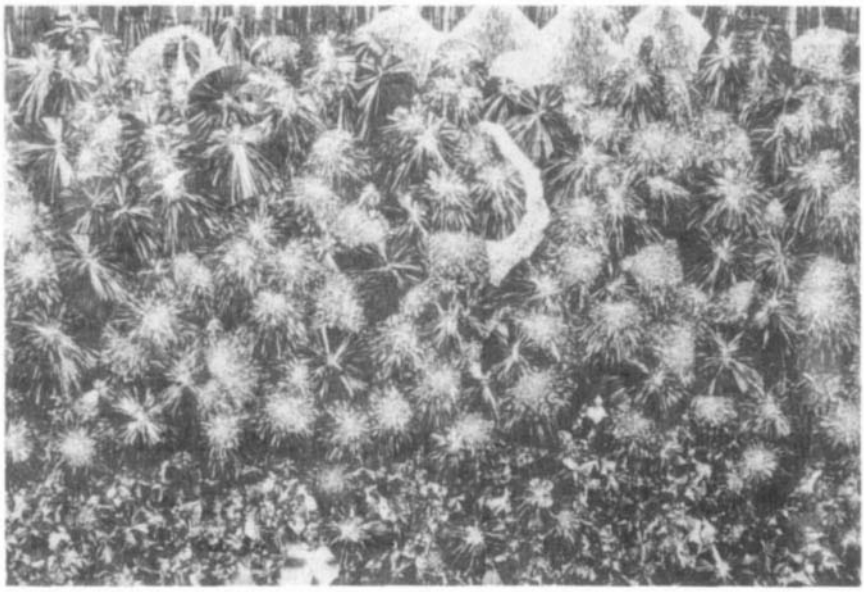

FIG. 2. Photograph taken from a microtome cut of a sample of an industrial polypropylene quenched at the upper side. The grass-like area indicates transcrystallization (i.e., layer growth from the quenched wall). This growth is hampered by spherulites which become larger with increasing distance. By a final quench, smaller spherulites are found at a still larger distance. This second transition is a check for the visual observation of the moving zone.

to Krobath and Liedauer [12, 13]. These authors also gathered data from other works where the growth speeds of spherulites were investigated under the microscope for a high and a low molecular weight polypropylene [14, 15] and where the speed of zone crystallization [16] was investigated. The conclusion is drawn that the movement of the crystallization front is governed by the same processes as the growth of spherulites. Accordingly, there is no influence of molecular weight or molecular weight distribution, as Magill has proven [17] except for very low molecular weights. Figure 4 shows that below 90°C a front movement can no longer be observed. At this high degree of supercooling the growth of a front is completely hampered by disperse crystallization in the melt. Finally, one observes that, at about 105°C, there is a maximum in growth speed. This agrees completely with the experiences of Magill and cooperators [18] and other investigators for spherulite growth.

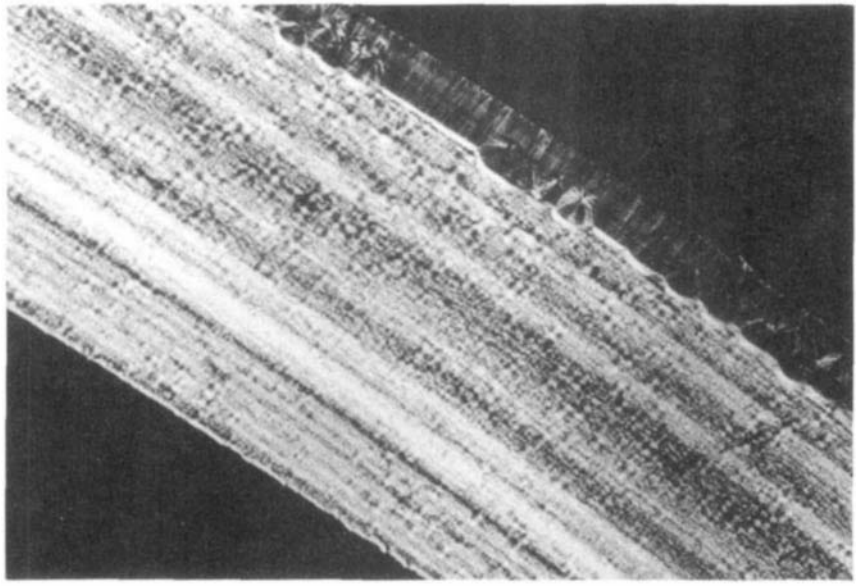

FIG. 3. Transcrystallized layer obtained when the second quench occurred before this layer was hampered by spherulite growth.

2.2. The Theory of Crystallization under Heat Transfer Conditions

Our interest should now be focused on the mechanisms leading to the formation of the zone. The existence of this zone was first predicted by Berger and Schneider [19] in a more global way. In the present context we prefer to derive this zone from the nucleation and growth mechanisms. For this purpose, a second paper by this group (Schneider, Köppl, and Berger [1, 2]) is of central importance. In this work, Avrami's integral equation [20], which is derived for isothermal crystallization at a fixed level of supercooling, is transformed into a set of differential equations ("rate equations") which can be integrated simultaneously with the energy equation (in our case the one-dimensional equation of heat conduction). One has

$$\xi = 1 - \exp(-\phi_0), \qquad \text{with}$$

$$\phi_0 = \frac{1}{V_\infty} \frac{4\pi}{3} \int_0^t \left[\int_z^t G(t')dt' \right]^3 dN'(z) \qquad (1)$$

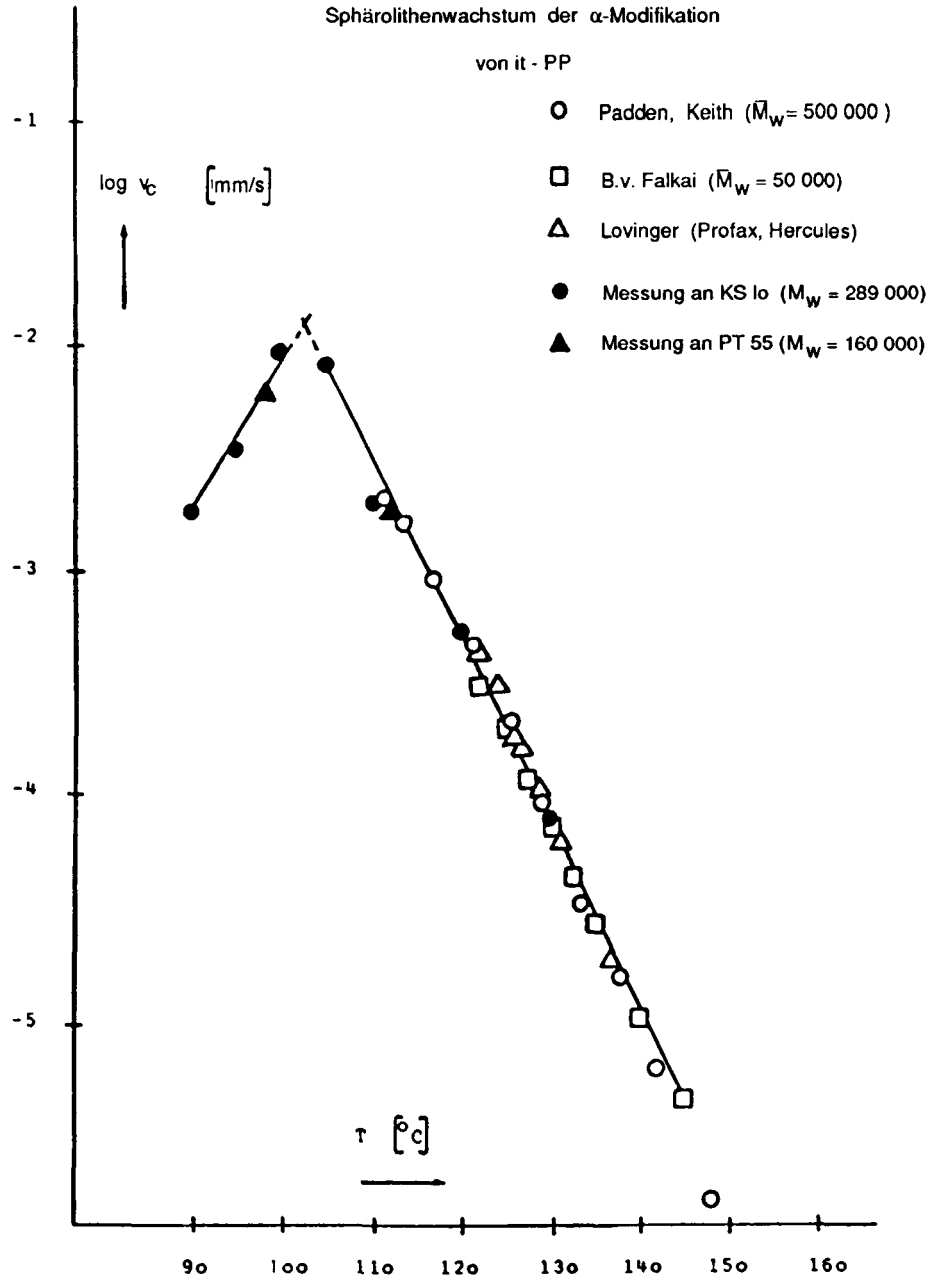

FIG. 4. Speed of the front of the transcrystallizing layer at the quenched wall temperature, according to Ref. 13. Below 90°C, wall temperature layer growth is completely hampered by spherulite growth in the melt. (●) Industrial reactor polypropylene. (▲) Industrial rheology controlled polypropylene. (○) High molar mass PP, spherulite growth. (□) Low molar mass PP, spherulite growth. (△) Zone crystallization. Courtesy of Alfred Hüthig Verlag, Heidelberg.

according to Avrami, with ξ the degree of crystallinity, ϕ_0 the "unrestricted" crystallinity, t the time, V_∞ the maximum achievable volume fraction of crystallites, G the linear growth speed of spherulites, and N' the number of activated nuclei per unit volume. By successive differentiation with respect to the time, one obtains the "rate equations":

$$\phi_1 = \frac{L}{G(T(t))}\frac{\partial\phi_0}{\partial t}, \qquad \phi_2 = \frac{L}{G(T(t))}\frac{\partial\phi_1}{\partial t}, \qquad \phi_3 = \frac{L}{G(T(t))}\frac{\partial\phi_2}{\partial t},$$

$$\phi_3 = \frac{N'(t)}{\overline{N}}, \qquad \text{with } L = \left(\frac{V_\infty}{6\overline{N}}\frac{3}{4\pi}\right)^{1/3} \tag{2}$$

with $\overline{N}$ the number of *potential* nuclei per unit volume and L an average distance between these nuclei. The equation for ϕ_3 holds for the special case where N' is a unique function of temperature T and depends on time only through the change of temperature with time. This assumption is not trivial, as will be shown later. In contrast, growth speed G can safely be considered as a unique function of temperature [$G(t) = G(T(t))$].

The equation of heat conduction used for our purpose reads:

$$\rho c\frac{\partial T}{\partial t} = \lambda\frac{\partial^2 T}{\partial x^2} + \rho h\frac{\partial\xi}{\partial t} \tag{3}$$

where ρ is the density, c is the heat capacity, λ is the heat conductivity, and h is the specific latent heat of crystallization. The integration starts with $\phi_3(T(t))$ and ends up with ϕ_0, which is translated into the real degree of crystallinity by the first Eq. (1). (This equation copes with the impingement of spherulites in a very convenient way.)

For this procedure we need $G(T)$ and $N'(T)$. For polypropylene, values of $G(T)$ can be deduced from Fig. 4. For the number of activated nuclei, the work of Van Krevelen and his group [21–23] is consulted. For this purpose, Fig. 5 is introduced. This figure shows the number of "induced" nuclei as a function of (reduced) temperature $\nu = (T_m - T)/(T_m - T_g)$, where T_m is the melting point and T_g is the glass transition temperature. The authors observed a kind of hysteresis loop. The lower branch is observed with decreasing temperature. By passing through the glass transition temperature many more nuclei are apparently formed, so that, with increasing temperature, the upper branch is found. But we

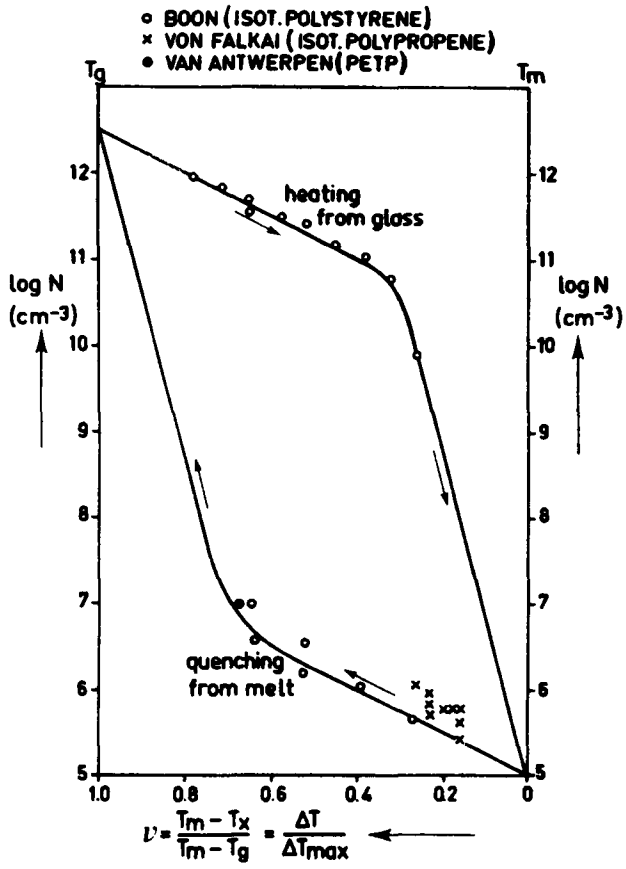

FIG. 5. Number of nuclei per unit of volume against reduced crystallization temperature $(T_m - T)/(T_m - T_g) = \nu$ according to Van Krevelen [23]. Courtesy of Brunner Verlag, Zürich.

are interested only in that part of the lower branch which shows the lower (negative) slope. From Figs. 4 and 5 we obtain the following equations valid in the temperature range of 105°C < T < 150°C, with a reference temperature T_r of 183°C:

$$G(T) = \alpha_r \exp\left[-\beta(T - T_r)\right] \tag{4}$$

with $\alpha_r = 2.05 \times 10^{-12}$ m/s and $\beta = 0.196\ \mathrm{K}^{-1}$, and

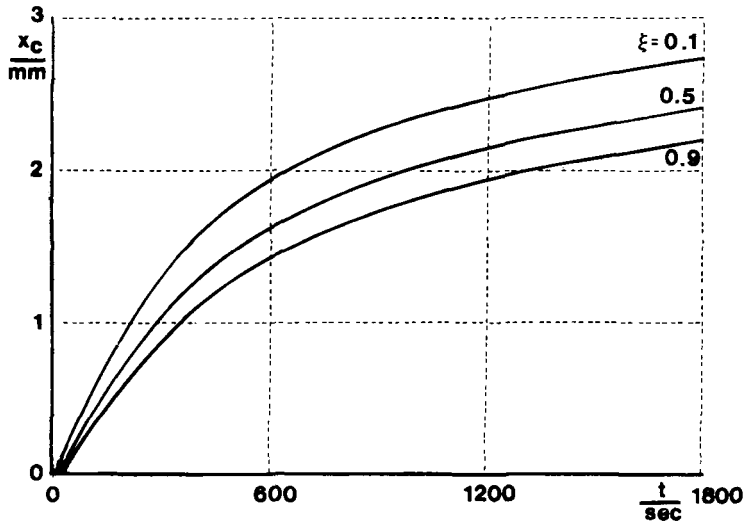

FIG. 6. Lines of constant crystallinity $\xi = 0.1$, 0.5, and 0.9 as functions of time for $T_i = 200°C$, $T_w = 110°C$, $\tilde{\alpha}_n = 10^{11}\ m^{-3}$, and $D = 10$ mm [approximate theory with uncoupled equation of heat conduction ($h = 0$)] [4]. Courtesy of Pergamon Press, Oxford.

$$N'(T) = \tilde{\alpha}_r \exp\left[-\tilde{\beta}(T - T_r)\right] \tag{5}$$

with $\tilde{\alpha}_r = 10^{11}\ m^{-3}$ and $\tilde{\beta} = 0.030\ K^{-1}$.

2.3. Some Experimental Support

From these data and the above-cited equations, the progress of the crystallization zone is calculated. For this purpose, a premelted disk of 10 mm thickness and large radius is considered. This disk is thought to be quenched on one side from initial temperature $T_i = 200°C$ to the "wall" temperature $T_w = 110°C$. In Fig. 6, curves for $\xi = 0.1$, 0.5, and 0.9 are plotted showing the fact that the zone becomes broader with increasing time and distance from the quenched wall. In Fig. 7, the wall temperature is varied for $\xi = 0.5$. At the same time, experimental points are inserted. One should keep in mind that no adjustments have been carried out. This means that agreement between theoretical and experimental points is reasonable. Full curves were calculated for $h = 0$, i.e., with the decoupled equation of heat conduction. The exact calculation

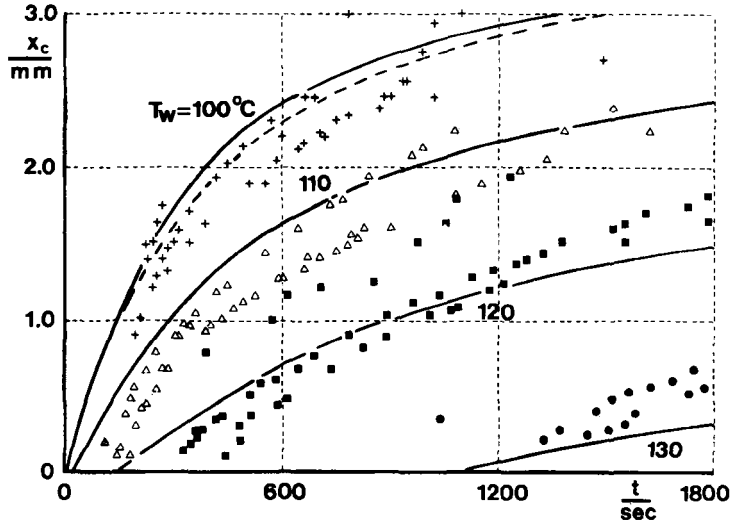

FIG. 7. Lines of constant crystallinity $\xi = 0.5$ as functions of time t and initial temperature $T_i = 200°C$ with varying quenched wall temperatures T_w for an industrial reactor PP. Full lines: Approximate theory with uncoupled equation of heat conduction ($h = 0$). Dashed line: Exact solution. Experimental points according to Mrs. E. Ratajski for industrial reactor PP [4]. Courtesy of Pergamon Press, Oxford.

gives the dashed line for $T_w = 100°C$. In view of the experimental spread, the improvement is not important.

A closer inspection shows that at short times of observation the experimental points lag behind the corresponding theoretical curves. In principle, this must be ascribed to the simplification made with respect to ϕ_3.

2.4. A Final Discussion

Actually, a temperature-dependent value of the number of activated nuclei N' can only be introduced by the assumption of an activation time spectrum. One must assume various activation processes (dependent on the varying surface properties of particles causing heterogeneous nucleation) with activation times τ_j of differing temperature dependences. In this way one obtains

$$\phi_3(T,t) = \frac{N'(T,t)}{\bar{N}} = \sum_j \frac{\bar{N}_j}{\bar{N}} a_j(T,t) \tag{6}$$

with

$$a_j(T,t) = 1 - \exp\left\{ - \int_0^t \frac{dt'}{\tau_j(T(t'))} \right\} \tag{7}$$

A value of N' depending merely on temperature is obtained with a simplified spectrum of the form

$$\tau_j(T) = \begin{cases} \infty, & T > T_j \\ 0, & T < T_j \end{cases} \tag{8}$$

when T_j is the temperature at which the jth process is activated without delay. If there is any delay which, in fact, may be expected from a physical point of view, one must also differentiate ϕ_3 with respect to time to enable a simultaneous integration.

One has:

$$\frac{\partial \phi_3}{\partial t} = \sum_j \frac{\bar{N}_j}{\bar{N}} \frac{1 - a_j(T(t),t)}{\tau_j(T(t))} \tag{9}$$

If there is only one mechanism, Eq. (9) reduces to

$$\frac{\partial \phi_3}{\partial t} = \frac{1}{\tau}(1 - \phi_3) \tag{10}$$

as proposed by Schneider et al. This equation can be integrated conveniently together with the equation of heat conduction, in contrast to Eq. (9). On the other side, no temperature-dependent number of "induced" nuclei can be introduced if only one mechanism is considered. However, as we can see from Fig. 7, the use of Eq. (5) gives almost correct results, so that an approximate treatment of Eq. (9) will certainly be found and will be sufficient for a sufficiently correct description of crystallization under general heat-transfer conditions in a quiescent polymer melt.

3. FLOW-INDUCED CRYSTALLIZATION

3.1. Introductory Remarks

Flow-induced crystallization is observed with melt spinning and with several other processing techniques. Despite the enormous amount of careful experimental work done in melt spinning [24] in order to elucidate crystallization processes, real progress in understanding has so far been achieved only with shearing experiments. For a survey of these latter experiments, see Ref. 4. In this paper you will also find a more extended discussion: According to an interesting paper by Zülle, Linster, Meissner, and Hürlimann [25], extensional flow at a constant rate of extension is nearly equivalent to shear flow at a shear rate increasing exponentially with time. As the flow in a spin-line is characterized by an extension rate increasing with the distance from the spinneret until crystallization occurs, it becomes quite clear that shearing experiments provide much milder conditions for a quantitative evaluation.

The occurrence of shear-induced crystallization is characteristic for the injection molding process [26–28]. In the cross-sections of the walls of injection molded articles, one finds highly oriented surface layers which are the consequence of this type of crystallization. Injection molding, however, is not a simple process. In Fig. 8 we find surface layers which are produced in a much more perspicuous way by short-time shearing at a constant level of supercooling in a duct of rectangular cross-section (with a large aspect ratio). We may consider this as nice texturing which has nothing to do with phase diagrams in the classical sense. Admittedly, such texturing is not always desirable. In injection molded articles it can cause warping and cleavability. From a practical point, it can be avoided by the use of narrow molecular weight distributed polymer samples. But this forms an entrance to our more fundamental considerations.

3.2. Experiments

How dangerous is it, however, to contend that shear-induced crystallization has really nothing to do with phase separation? This became obvious on the basis of experiments carried out by Rietveld and McHugh [29] and Wolff et al. [30]. These authors showed that prior to extension and shear-induced crystallization, respectively, a kind of phase separation occurs in polymer solutions. Extensive thermodynamic considera-

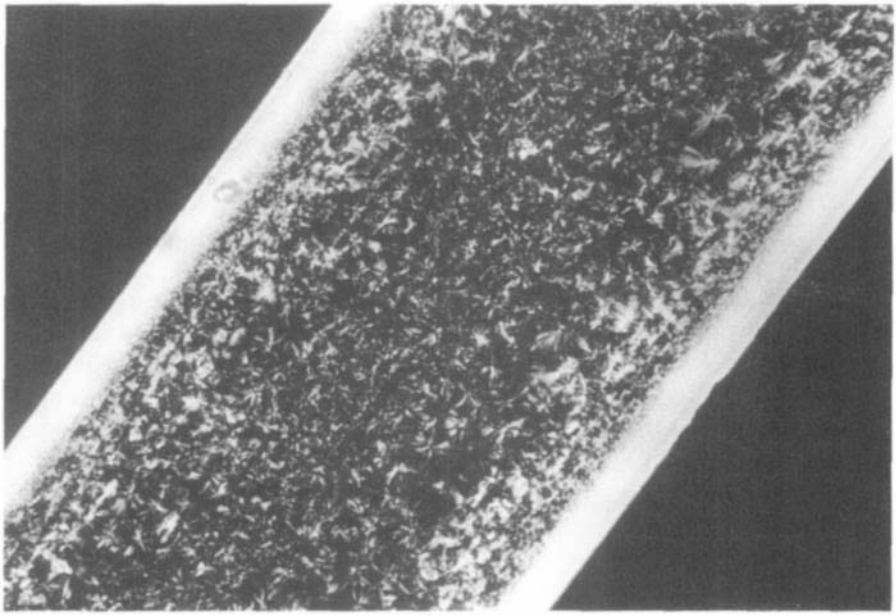

FIG. 8. Highly oriented surface layers as obtained according to the method described in Section 3.1. Shearing time 2 s, shear rate at duct wall 100 s^{-1}, level of supercooling 150°C, industrial reactor PP.

tions were devoted to this phenomenon [31]. On the other hand, no direct observations confirmed this kind of phase separation for polymer melts. Interestingly enough, however, a type of quenching experiments introduced by one of the present authors and his coworkers [12, 13, 32] gave evidence that something happens in the flowing melt (in particular, in the sheared melt) even at temperatures well above the melting point. If such a melt is quickly quenched to a sufficiently low temperature, shear-induced crystallization occurs, with all the characteristics of a texture containing strings of highly oriented crystalline material. These characteristics cannot possibly be formed during the quench, as flow is stopped prior to this cooling operation. On the other hand, if the material is kept for varying times at the temperature level of the shearing before it is quenched, the proneness to shear-induced crystallization gradually decreases: The material relaxes. If the birefringence of the quenched material is plotted against the tempering time, one finds an

TABLE 1. Relaxation Times of the Precursors to Shear-Induced Crystallization at Various Flow Temperatures (according to Wippel [33]) for an Industrial Polypropylene

Temperature, °C	Relaxation time, s
210	0.83
205	3.67
200	7.27
195	15.88
190	57.81

exponential decay, from which a relaxation time can be deduced. This has been shown by Wippel [33].

For an industrial polypropylene, this relaxation time is presented for a temperature range of shearing between 210 and 190°C in Table 1. Above 210°C the relaxation time is too short for this type of experiment; below 190°C the melt shows flow anomalies. In Fig. 9 the logarithm of the zero shear viscosity of the polymer melt is plotted against the logarithm of this relaxation time. One notices that the temperature dependence of the relaxation time is much higher than the one of the viscosity. This means that with this relaxation much more happens than just a redistribution of chain segments in an ordinary melt, as governed by the WLF equation [34]. As is well known, this equation holds for the temperature dependence of the zero shear viscosity. On the other hand, the changes in the sheared melt must be very small. They cannot be detected by flow birefringence [32] and other, probably less sensitive, rheological measurements.

3.3. Theoretical Considerations

A model containing the minimum number of parameters was introduced [3, 4] by the following differential equation:

$$\tau \dot{\Phi} = \left(\frac{\dot{\gamma}}{\dot{\gamma}_a}\right)^2 (1 - \Phi) - \Phi \tag{11}$$

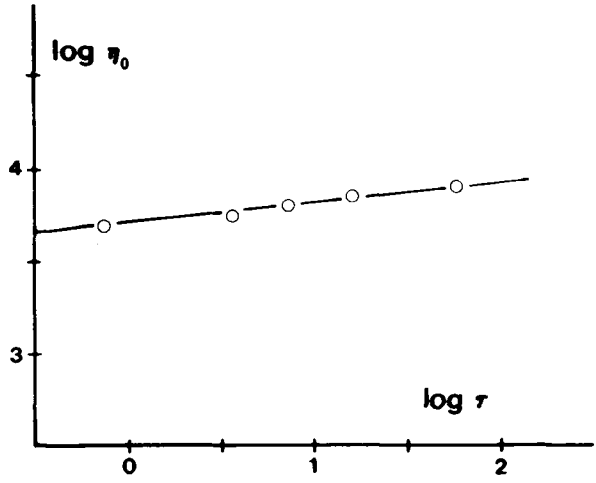

FIG. 9. Double logarithmic plot of zero-shear viscosity η_0 against relaxation time τ of proneness to shear-induced crystallization. Experiments on industrial reactor PP, according to Wippel [4]. Courtesy of Pergamon Press, Oxford.

where Φ is the probability for the formation of shear-induced structures, τ is the relaxation time, and $\dot{\gamma}_a$ is the critical shear rate of activation. The first term on the right-hand side is the creation term, the second one is the decay term, which becomes clear when the equation is divided by τ. As a third parameter, besides τ and $\dot{\gamma}_a$, a combined nucleation and growth factor

$$\hat{g}(T) = \sqrt[4]{g_1 g_2 g_3 g_n} \tag{12}$$

is introduced, which has the dimension of reciprocal seconds. In this relation the nucleation factor is introduced by

$$G_n = g_n \Phi, \text{ with } G_n \text{ comparable to } \dot{N}' \tag{12a}$$

whereas the growth factors (of three-dimensional growth) are defined by

$$G_i = g_i \Phi, \text{ with } i = 1, 2, 3 \tag{12b}$$

Because of Eq. (12), we called this model the "model of uttermost unifor-

mity." Since, according to Eq. (11), Φ always increases linearly with time at the beginning of the shearing treatment, the Avrami exponent is enhanced above the usual values for quiescent melts. In fact, if for simplicity we consider the growth of an orthorhombic crystallite, we have for "unrestricted" crystallinity

$$\phi_0 = 8 \int_0^t \prod_i \left[\int_s^t G_i(z)dz \right] G_n(s)ds \tag{13}$$

If the G_i's and the G_n are constants, one has

$$\phi_0 = 8G_nG_1G_2G_3 \int_0^t \left[\int_s^t dz \right]^3 ds = 2G_nG_1G_2G_3t^4 \tag{14}$$

Avrami's corresponding equation for the isothermal growth of sperulites in a quiescent melt is

$$\phi_0 = \frac{\pi}{3} G_nG^3t^4 \tag{14a}$$

Inserting this expression into the first Eq. (1), one has

$$\xi = 1 - e^{-kt^4}$$

with Avrami's exponent equal to 4. When shearing at a constant shear rate begins at time zero, Eqs. (12a) and (12b) are needed. In a first approximation with respect to (t/τ), the solution of Eq. (11) reads

$$\Phi \simeq \left(\frac{\dot{\gamma}}{\dot{\gamma}_a}\right)^2 \frac{t}{\tau} \tag{15}$$

Inserting this linear function into Eqs. (12a) and (12b) and using the obtained expressions in Eq. (13), one finds

$$\phi_0 = 8g_1g_2g_3g_n \int_0^t \left[\int_s^t \phi(z)dz \right]^3 \phi(s)ds$$

$$= 2\hat{g}^4 \left[\int_0^t \phi(s)ds \right]^4$$

$$= 2\hat{g}^4 \left[\left(\frac{\dot{\gamma}}{\dot{\gamma}_a}\right)^2 \frac{t^2}{2\tau}\right]^4 \propto t^8 \tag{16}$$

The doubling of the Avrami exponent is due to the integrals $\int t dt$ occurring in Eq. (16), which are the consequence of the initially linear increase of Φ. If the model has a lower degree of "uniformity," one obtains a lower value for the enhanced Avrami exponent. Interestingly enough, Sherwood, Price, and Stein [35] found increasing Avrami exponents with increasing shear rates. This phenomenon finds its natural explanation in our theory.

In order to evaluate the parameters $\dot{\gamma}_a$ and τ, a variety of experiments were designed and partly carried out, like Wippel's experiment mentioned above. A more detailed description is given in Ref. 4. As one heavily relies on these experiments in the quenching procedure, these parameters can, in principle, only be determined for a range of relatively high temperatures where no crystallization occurs. Parameter $\hat{g}$, which is certainly also a strong function of temperature, is zero in this temperature range. Separate values for $\dot{\gamma}_a$ and τ can be obtained for the lower temperatures only by extrapolation. From Table 1 and Fig. 9, however, we can deduce that τ must be rather large at temperatures where crystallization really happens during shearing. This means that Eq. (15) can probably be used in many cases of industrial relevance.

Under this condition, the phenomenon of shear-induced crystallization is governed by a single combined and dimensionless parameter:

$$P = \dot{\gamma}_a \left(\frac{\tau}{\hat{g}}\right)^{1/2} \tag{17}$$

At the same time, the induction time after uninterrupted shearing becomes

$$t_i = (8 \ln 2)^{1/8} P \dot{\gamma}^{-1} \tag{18}$$

This means that the total critical shear $\gamma_i = t_i \dot{\gamma} = (8 \ln 2)^{1/8} P$ becomes independent of shear rate $\dot{\gamma}$. This is a limiting law observed by Lagasse and Maxwell [36] for polyethylene melts in a wide range of shear rates even at low levels of supercooling.

Some remarks should be made with respect to the description of nonisothermal situations, such as those occurring under realistic processing

conditions. In partial analogy to Eqs. (2), which are valid for quiescent melts, one finds the following set of rate equations (see Ref. 4):

$$\psi_0 = \left(\frac{\phi_0(t)}{2}\right)^{1/4} = \int_0^t \hat{g}(T(z))\Phi(z)dz$$

$$\frac{1}{\hat{g}(T(t))}\frac{\partial\psi_0}{\partial t} = \psi_1, \qquad \frac{\partial\psi_1}{\partial t} = \left(\frac{\dot{\gamma}}{\dot{\gamma}_a}\right)^2\frac{1-\psi_1}{\tau} - \frac{\psi_1}{\tau} \tag{19}$$

One can recognize without difficulty that ψ_1 is the same as our probability function Φ. However, ψ_0 is not the "unrestricted" crystallinity ϕ_0 but the fourth root of one-half of this quantity. The last rate equation is identical with Eq. (11). The lower number of rate equations is not due to the lower dimensionality of the growth processes. It is a consequence of the combined treatment indicated by Eq. (12). In the case of the quiescent melt, a further differentiation of ϕ_3 with respect to time caused difficulties because of the nature of the relaxation time spectrum. Here the analogous differentiation of ϕ_1 did not cause any problem because shear-induced crystallization is considered as the consequence of homogeneous nucleation by the action of shear. No spectrum is expected. In view of the difficulties expected in practical calculations, where, beside the convection of heat the convection of nucleated fluid is also expected, the simpler structure of Eqs. (19) can only be welcomed.

In view of the experience with isothermal crystallization at constant levels of supercooling, one would expect that the last term in the equation for $\partial\psi_1/\partial t$ could be omitted. (Compare Eq. 15.) A stepwise integration, occurring simultaneously with the equation of heat conduction, shows that—with the simplified equation for $\partial\psi_1/\partial t$—the parameters $\dot{\gamma}_a$ and τ remain combined. Unfortunately, this does not hold for $\hat{g}$, which enters only in the second step of the integration. As a consequence, the determination of parameter P at several levels of supercooling in isothermal experiments will not suffice for the evaluation of the necessary model parameters. Special quenching experiments are planned where, in simple words, $\dot{\gamma}_a$ and τ correspond to the higher temperature, whereas $\hat{g}$ corresponds to the lower one.

3.4. Experiments with Interrupted Shear

An interesting field of experiments which considerably widens the horizon of possibilities is that of interrupted shearing. According to the presented theory, a period of shearing much shorter than the above-

mentioned induction time t_i causes subsequent shear-induced crystallization. A very realistic experiment has been carried out in a slit die (a duct with a rectangular cross-section with a large ratio) by Liedauer [37]. (See also Ref. 4.) Near the end of this rather long duct, windows were placed in opposite positions in the large side walls. Through these windows the optical path difference, as caused by varying birefringence effects, could be observed continuously by the use of a special optical arrangement. The duct was filled isothermally with a melt of an industrial polypropylene from a screw extruder. Because the die is thermally insulated from the extruder, its temperature can easily be lowered by the circulation of a heat transfer fluid to a level below the melting point. Levels of relatively low supercooling are chosen where normal crystallization takes a long time to appear. At time zero, extrusion is suddenly started again at a constant extrusion pressure for variable periods of time t_s shorter than t_i. During these periods, flow birefringence is observed. After cessation of flow, this birefringence does not disappear completely. This indicates the sporadic start of shear-induced crystallization (crosslinking of oriented molecules). The observed path difference, which increases drastically at later times, reflects the massive growth of a shear-induced crystalline layer. The proportionality factor between layer thickness and path difference is determined by shear rate and shearing time applied during the previous period of shearing. With these experiments the consequences of the theory can be checked successfully. This is the first on-line measurement of layer growth.

In Fig. 10 the results for five shearing times—chosen to be extremely short compared with the times of observation—are shown for an apparent shear rate $\dot{\gamma}_A = 100\ s^{-1}$ at the (large) duct walls. With the use of the fundamental equations of the previous section, a theoretical prediction of layer growth was developed. The full lines in Fig. 10 are fitted to the experimental points by adjustment of parameter P. In this way, for all curves, the same induction time t_0 at the wall, corresponding to the chosen $\dot{\gamma}_A$, was obtained within an acceptable spread ($t_0 = 16 \pm 0.5$ s, $P \cong 0.16$). One may observe that this t_0 is much longer than the chosen shearing times. The theoretical lines start at times $\hat{t}_0 > t_0$, indicating the delayed moment when crystallization (massively) starts at the wall, if $t_s < t_0$. Apparently some flow birefringence arrested by a beginning crosslinking obscures this effect in the experimental points, the onset of crystallization being identified in the theory with the half conversion time, when crystallization rigorously progresses. As this work is still not completed, further discussion must be postponed. Measurements in

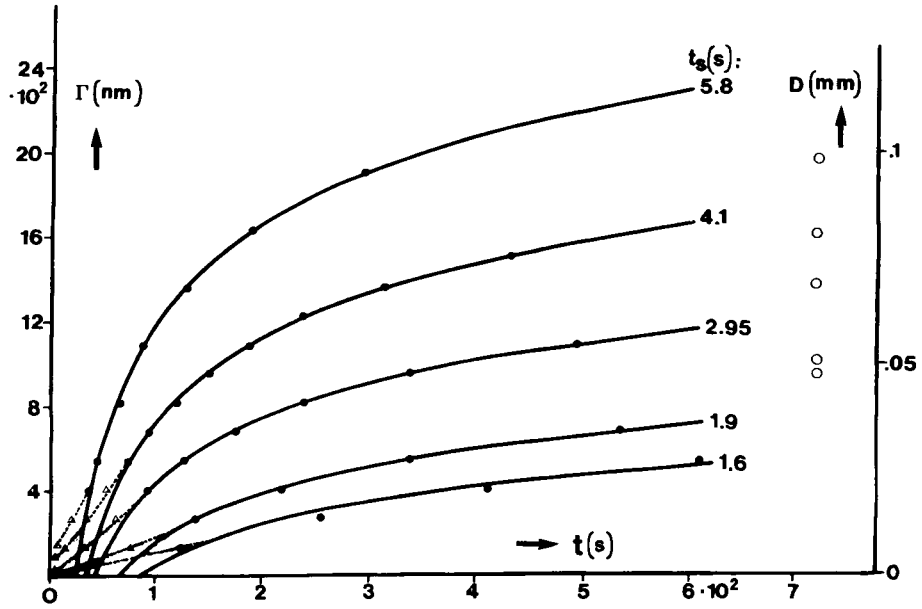

FIG. 10. Optical retardation Γ against time t for five shearing times t_s at an apparent shear rate $\dot{\gamma}_A = 100\ s^{-1}$ at the wall of the duct for an industrial reactor PP. Full lines adapted to the experimental points according to the described theory with $t_0 = 16 \pm 0.5$ s. Dotted lines connect early experimental points where the flow birefringence of previous shear flow seems arrested by starting crosslinking by crystallization. The ultimate layer thicknesses from microtome cuts are on the right-hand side [4]. Courtesy of Pergamon Press, Oxford.

ducts with continuously decreasing wall temperatures (at a constant cooling rate) may lead to a separation of $\hat{g}(T)$, as indicated above.

It probably should be mentioned that Fig. 8 is taken from a sample in which the shear-induced layers were obtained in the way described in this last section. They are much neater than those usually obtained in injection-molded samples.

4. CONCLUSIONS

Both types of crystallization which occur under heat transfer conditions in polymer processing, viz., spherulitic and shear-induced fibrillar

crystallization, can now be considered as well understood from a phenomenological point of view.

However, there are still difficulties in the experimental field with respect to the determination of all the data required for the calculations. Progress has been made in the design of proper experiments, but most data were obtained for one industrial polypropylene.

As there is a variety of other semicrystalline polymers of potential interest, a molecular theory predicting at least some of the required data in terms of molecular weight distribution or molecular structure would be desirable.

ACKNOWLEDGEMENT

This work was sponsored by the Austrian "Fonds zur Förderung der wissenschaftlichen Forschung," Vienna, under Contract S 33 02.

REFERENCES

[1] W. Schneider, A. Köppl, and J. Berger, *Int. Polym. Process. II*, p. 151 (1988).

[2] J. Berger, "Erstarren von Kunststoffen unter dem Einfluss von Wärmeleitung und Kristallisationskinetik," Doctoral Thesis, Vienna University of Technology, February 1988.

[3] G. Eder and H. Janeschitz-Kriegl, *Colloid Polym. Sci., 266*, 1087 (1988).

[4] G. Eder, H. Janeschitz-Kriegl, and S. Liedauer, "Crystallization Processes in Quiescent and Moving Polymer Melts under Heat Transfer Conditions," *Prog. Polym. Sci., 15*, 629 (1990).

[5] D. J. Walsh, J. S. Higgins, and A. Maconnachie (eds.), *Polymer Blends and Mixtures*, Nijhoff, Dordrecht, 1985.

[6] D. R. Paul and S. Newman (eds.), *Polymer Blends*, Vols. 1 and 2, Academic, San Diego, 1978.

[7] J. J. Elmendorp, "A Study on Polymer Blending Microrheology," Doctoral Thesis, Delft University of Technology, 1986.

[8] H. L. Goldsmith and S. G. Mason, in *Rheology, Theory and Application*, Vol. 4 (F. R. Eirich, ed.), Academic, New York, 1967, p. 141.

[9] J. Stefan, *Ann. Phys. Chem. (Wiedemann), M.F. 42*, 269 (1891).

[10] J. Crank, *Free and Moving Boundary Problems*, Clarendon Press, Oxford, 1984.
[11] G. Eder and H. Janeschitz-Kriegl: *Polym. Bull., 11*, 93 (1984).
[12] H. Janeschitz-Kriegl, G. Eder, G. Krobath, and S. Liedauer, *J. Non-Newtonian Fluid Mech., 23*, 107 (1987).
[13] H. Janeschitz-Kriegl, R. Wimberger-Friedl, G. Krobath, and S. Liedauer, *Kautsch. Gummi, Kunstst. 40*, 301 (1987).
[14] B. von Falkai, *Macromol. Chem. 41*, 86 (1960).
[15] F. J. Padden and H. D. Keith, *J. Appl. Phys. 30*, 1485 (1959).
[16] A. J. Lovinger, J. O. Chua, and C. C. Gryte, *J. Polym. Sci., Polym. Phys. Ed., 15*, 641 (1977).
[17] A. Gandica and J. H. Magill. *Polymer, 13*, 595 (1972).
[18] H. J. Magill, *J. Appl. Phys., 35*, 3249 (1964); *J. Polym. Sci., Part A2, 5*, 89 (1967).
[19] J. Berger and W. Schneider, *Plast. Rubber Process. Appl., 6*, 127 (1986).
[20] M. Avrami, *J. Chem. Phys., 7*, 1103 (1939); *8*, 212 (1940); *9*, 177 (1941).
[21] J. Boon, G. Challa, and D. W. Van Krevelen, *J. Polym. Sci., Part A2, 6*, 1791 (1968).
[22] J. Boon, G. Challa, and D. W. Van Krevelen, *Ibid., 6*, 1835 (1968).
[23] D. W. Van Krevelen, *Chimia, 32*, 279 (1978).
[24] J. L. White and M. Cakmak, *Adv. Polym. Technol., 6*, 295 (1986).
[25] B. Zülle, J. J. Linster, J. Meissner, and H. P. Hürlimann, *J. Rheol., 31*, 583 (1987).
[26] M. R. Kantz, H. D. Newman, and F. H. Stigale, *J. Appl. Polym. Sci., 16*, 1249 (1972).
[27] D. R. Fitchmun and Z. Mencik, *J. Polym. Sci., Polym. Phys. Ed., 11*, 951 (1973).
[28] Z. Mencik and D. R. Fitchmun, *Ibid., 11*, 973 (1973).
[29] J. Rietveld and A. J. McHugh, *J. Polym. Sci., Polym. Lett. Ed., 21*, 919 (1983).
[30] M. N. Layec Raphalen and C. Wolff, "The Influence of Polymer Additives on Velocity and Temperature Fields," *IUTAM Symposium*, Essen 1984, p. 143.
[31] A. J. McHugh, E. P. Vrahopoulou, and B. J. Edwards, *J. Polym. Sci., Polym. Phys. Ed., 25*, 953 (1987).
[32] G. Eder, H. Janeschitz-Kriegl, and G. Krobath, *Prog. Colloid Polym. Sci., 80*, 1 (1989).
[33] H. Wippel, Report Delivered in Fulfillment of the Requirements for the Degree of a Diplom-Ingenieur at Linz University, 1989.

[34] J. D. Ferry, *Viscoelastic Properties of Polymers*, 3rd ed., Wiley, New York, 1980.
[35] C. H. Sherwood, F. P. Price, and R. S. Stein, *J. Polym. Sci., Polym. Symp.*, *63*, 77 (1978).
[36] R. R. Lagasse and B. Maxwell, *Polym. Eng. Sci.*, *16*, 189 (1976).
[37] S. Liedauer, Doctoral Thesis, Linz University, In Preparation.